



## Thermal shock, tribological and mechanical properties of micro and nano structured zirconia partially stabilized with yttria and ceria

*Dragomirescu Alina<sup>1</sup>, Botan Mihail<sup>1</sup>, Manoliu Victor<sup>1</sup>, Ionescu Gheorghe<sup>1</sup>, Stefan Adriana<sup>1</sup>, Mihailescu Alexandru<sup>1</sup>*

*<sup>1</sup>National Institute for Aerospace Research "Elie Carafoli" Bucharest, Materials Unit, 220 Iuliu Maniu Blvd, 061126 Bucharest, Romania*

[botan.mihail@incas.ro](mailto:botan.mihail@incas.ro)

### ABSTRACT

Plasma sprayed micro and nano-structural zirconia coatings were investigated under thermal shock and evaluation of tribological and mechanical properties. Tribological performances of coatings were investigated by stainless steel ball against coated disk testing procedure under dry friction conditions. Better wear performance of the nano-structured zirconia stabilized with yttria (7.5YSZ) is due to the microstructure and mechanical properties enhancements compared with micro structured coating stabilized with ceria (CSZ). Advantages of nano-structured zirconia (7.5YSZ) coating were observed under thermal shock compared with ceria stabilized (CSZ) coating. Thermal shock was performed under quick heating and cooling of Nimonic-90 based alloy coated samples with a heat and cooling maximum gradient about of 100C°/s using a dedicated installation from INCAS. The SEM structural investigation showed a complex microstructure. SEM images of plasma sprayed micro (CSZ) and nano (7.5YSZ) structured zirconia present well and partially melted splats and areas. A higher thermal shock resistance, tribological and mechanical properties were found on nano-structured zirconia coatings stabilized with yttria, this effect was correlated by nano structured areas in coating microstructure and the presence of melted splats.

**KEYWORDS: ZIRCONIA, CERIA, TBC, THERMAL SHOCK, TRIBOLOGY**

### NOMENCLATURE

*A* – Contact area, mm<sup>2</sup>  
*C<sub>p</sub>* - heat capacity, (Jg<sup>-1</sup>K<sup>-1</sup>)  
*d* - Arithmetic mean of the two diagonals, d1 and d2 in mm  
*D<sub>th</sub>* - thermal diffusivity, (m<sup>2</sup>s<sup>-1</sup>)x10<sup>-6</sup>  
*E* - Young's modulus, elastic modulus, GPa  
*F* – Load in kgf  
*F(N)* - normal applied force, N,  
*H* - nano, micro, macrohardness, kg/mm<sup>2</sup>, GPa  
*H<sub>v</sub>* - Vickers hardness number, kg/mm<sup>2</sup>, GPa  
*L* - sliding distance, m  
*T<sub>m</sub>* - melting point, (K)  
*W* - Wear  
*W<sub>m</sub>* – Massic wear

#### *Greek Symbols*

*α* - thermal expansion coefficient, (K<sup>-1</sup>)x10<sup>-6</sup>  
*Δ<sub>m</sub>* - mass loss at the end of the test, mg  
*λ* - thermal conductivity, Wm<sup>-1</sup> K<sup>-1</sup>  
*ν* - Poisson's number,

#### *Subscripts*

*m* – mass, melting  
*th.* - thermal  
*V* - Vickers

## 1 Introduction

Thermal Barrier Coating (TBC) materials are widely used as thermal protection systems. There are many application of (TBC) from aerospace, turbine engine to nuclear [1]–[5]. Modern Aircraft industry aimed in using of gas turbine engines to get higher temperatures for improving the efficiency and reduction of CO<sub>2</sub> emission. In this respect, researchers focused on developing more efficient Thermal Barriers Coatings (TBCs) and associated technics of deposition to protect metallic alloys components. Depending on application of TBC's and regarding the technology readiness level, there were developed several techniques of deposition, such as Atmospheric Plasma Spraying (APS), High Velocity Oxy-Fuel (HVOF), Electron Beam-Physical Vapor Deposition (EB-PVD) and Plasma Spray-Physical Vapor Deposition (PS-PVD). The last two seemed the most performant due to the special columnar structure of the resulted coating [3], [5], [6]. Given the TBC's applications, numerous factors for achieving a good protection system such as: powder morphology, pre-treatment of the metal substrate, bond coat solutions, type of coating method, were taken into account.[3], [4], [7].

Currently, most of TBCs are based on Yttria Stabilized Zirconia (YSZ) and are commonly applied using the Atmospheric Plasma Spraying (APS) and Electron Beam Physical Vapor Deposition (EB-PVD) techniques [5], [8], [9]. Several authors reported that the addition of CeO<sub>2</sub> into YSZ coating is supposed to be effective for the improvement of thermal cycling life regarding its higher thermal expansion coefficient and a lower thermal conductivity than YSZ [1], [3], [5], [10], [11].

In literature some other rare earth oxides as stabilizers of ZrO<sub>2</sub> besides Y<sub>2</sub>O<sub>3</sub> and CeO<sub>2</sub> have been reported, such as Dy<sub>2</sub>O<sub>3</sub>, Nd<sub>2</sub>O<sub>3</sub>, Er<sub>2</sub>O<sub>3</sub>, Sm<sub>2</sub>O<sub>3</sub>, Yb<sub>2</sub>O<sub>3</sub>, Sc<sub>2</sub>O<sub>3</sub>, Gd<sub>2</sub>O<sub>3</sub>, Ta<sub>2</sub>O<sub>5</sub>, Nd<sub>2</sub>O<sub>5</sub>[3], [11]. Stabilizers used for TBC coatings are characterized by different level of stabilizing ability and stabilizing mechanisms which are correlated with the ability at high temperature of cation migration [3], [11]. Furthermore, new promising TBC material based on zirconia are doped by different rare-earth cations. These additions lead to the formation of dopant systems such as in the ZrO<sub>2</sub>–Y<sub>2</sub>O<sub>3</sub>–Nd<sub>2</sub>O<sub>3</sub>(Gd<sub>2</sub>O<sub>3</sub>, Sm<sub>2</sub>O<sub>3</sub>)–Yb<sub>2</sub>O<sub>3</sub>(Sc<sub>2</sub>O<sub>3</sub>) system which lead in reduction of the thermal conductivity [5]. In Table 1 are represented some TBC solutions and their properties.

**Table 1: Some properties for TBC solutions [3]–[6], [11], [12]**

Materials	T <sub>m</sub> (K)	D <sub>th</sub> (m <sup>2</sup> s <sup>-1</sup> )x10 <sup>-6</sup>	λ (Wm <sup>-1</sup> K <sup>-1</sup> )	α (K <sup>-1</sup> )x10 <sup>-6</sup>	E (GPa)	C <sub>p</sub> (Jg <sup>-1</sup> K <sup>-1</sup> )	ν
ZrO <sub>2</sub>	2953	0.43	2.17	15.3	21		0.25
8YSZ (APS)	2680	-	2.20-2.50	10.3-11	40	0.64	0.22
CeO <sub>2</sub>	2873	0.86	2.77	13	172	-	0.27-0.31
La <sub>2</sub> Zr <sub>2</sub> O <sub>7</sub>	2573	0.54	1.58	9.1	175	0.49	-
La <sub>2</sub> Ce <sub>2</sub> O <sub>7</sub>		0.19	0.6	12.3		0.43	-
CaZrO <sub>3</sub>	2550		2	8.4-8.9	149.3		0.28
BaZrO <sub>3</sub>	2963	1.25	3.42	8.1	181	0.45	-
SrZrO <sub>3</sub>	2883	1.4	2.08	10.9	170	0.46	0.25
Mullite	2123	-	3.3	5.3	30	-	0.25

*D<sub>th</sub>, thermal diffusivity; E, Young's modulus; α, thermal expansion coefficient; λ, thermal conductivity; C<sub>p</sub>, heat capacity; ν, Poisson's number; T<sub>m</sub>, melting point.*

In the current research, the thermal shock, tribological and mechanical behavior of ZrO<sub>2</sub>7.5%Y<sub>2</sub>O<sub>3</sub> and ZrO<sub>2</sub>24%CeO<sub>2</sub>2.5%Y<sub>2</sub>O<sub>3</sub> coatings made by APS technique, were tested and compared in the as-sprayed state. Tribological tests were performed using CETR UMT-universal tribometer, utilizing the module ball on ring under dry regime. Thermal shock tests were performed on a dedicated installation conceived by INCAS namely QTS-2-(Quick Thermal Shock) and hardness testing were performed using Vikers indentation method.

## 2 Samples and powder description.

Coatings were carried out onto Nimonic 90 substrates with zirconia based ceramic, stabilized with nano yttria and ceria powders over a bond coat MeCrAlY commercially named AMDRY 997.

The samples were coated by High Velocity Oxy-Fuel (HVOF) technique for bond coat (BC) and for top coat (TC) Air Plasma Spraying (APS) technique was used. Corresponding spraying conditions are described in Table 3. Two types of zirconia doped powders were used, hereinafter namely: INFRAMAT ( $ZrO_2 7.5\% Y_2O_3$  - nanostructured powder = 7.5YSZ) and M205NS ( $ZrO_2 25\% CeO_2 2.5\% Y_2O_3$  – ceria stabilized zirconium oxide powder = CSZ) with powder characteristics presented in Table 2. Ceria stabilized zirconium oxide M205NS ( $ZrO_2 25\% CeO_2 2.5\% Y_2O_3$ ) have a 2,5% of  $Y_2O_3$ , this coating solution surpasses the cyclic and thermal fatigue resistance of common 8% yttria stabilized zirconia ( $8 Y_2O_3 ZrO_2$ ) [13]–[15].

**Table 2: Nominal powder characteristics[13]–[15].**

Materials	Particle size	Chemical formula	Density	Service temperature	Trade name
INFRAMAT (7.5YSZ)	30-60 nm	$ZrO_2 7.5\% Y_2O_3$	6.10 g/cm <sup>3</sup>	1345°C (2450°F)	4039ON- 8601
M205NS (CSZ)	+11-125 μm	$ZrO_2 25\% CeO_2 2.5\% Y_2O_3$	5.3 – 5.5 g/cm <sup>3</sup>	1250 °C (2280 °F)	Metco 205NS

In table 3, powders and associated parameters for coatings using METCO 7M installation (Plasmajet s.r.l, Bucharest, Romania) are presented.

**Table 3: Spraying parameters used to perform top coat structures by APS.**

Nr.crt	Powder type	Gun	Thickness [mm]	Debit Ar/H2	I[A]	U[V]	Injector	Nozzle	Distance [mm]
1	$ZrO_2 25\% CeO_2 2.5\% Y_2O_3$	7MB	0.1-0.2	120/12	600	65	#2	SM6mm	100
2	$ZrO_2 7.5\% Y_2O_3$	7MB	0.1-0.2	120/12	600	65	#2	SM6mm	120

For bond coat (BC), HVOF deposition technique was used. The parameters for HVOF coating are: distance 230 mm, Substrate cooling was ensured by compressed air, oxy-fuel: oxygen and propylene, with flow rate for  $O_2=3410\text{mm}^3/\text{sec}$  and for propylene  $O_2=1488\text{mm}^3/\text{sec}$ , feed rate for bond coat powder 0.315g/sec.

The sample geometry dimensions are 30x50x2 mm for Nimonic90 substrate. The thickness of the bond coat (BC) deposition was about 45-70 μm and 270-310 μm for the top coat (TC).

### 3 Testing methods and results

#### 3.1 Tribological testing

In order to investigate the tribological behavior of investigated coatings, testing was performed by using of the CETR UMT-universal tribometer (Figure 1). Tests were performed with the ball on ring module under dry regime. The reason of this testing type selection was to investigate the mechanism of wear using as a counterpart a steel ball, the ball composition is according to- STAS 1456 11250 CS 200, Rul 1 DIN 100Cr6.

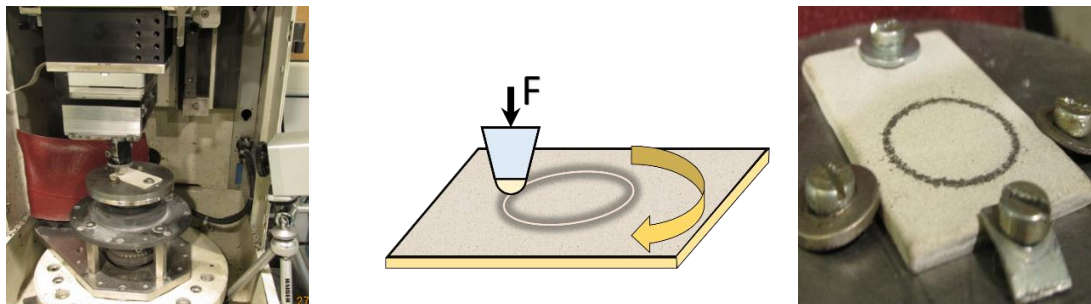


**Figure 1 Arrangement of the sample and principles of ball on disk testing method.**

Testing conditions are: Normal Force=10N, sliding speed=0.25m/s, sliding distance =100 m. (sliding radius =10mm, ball diameter =4.9 mm,  $w=238.735\text{rot/min}$ . The test was performed under controlled ambient temperature which was about 25°C all the time during testing performance.

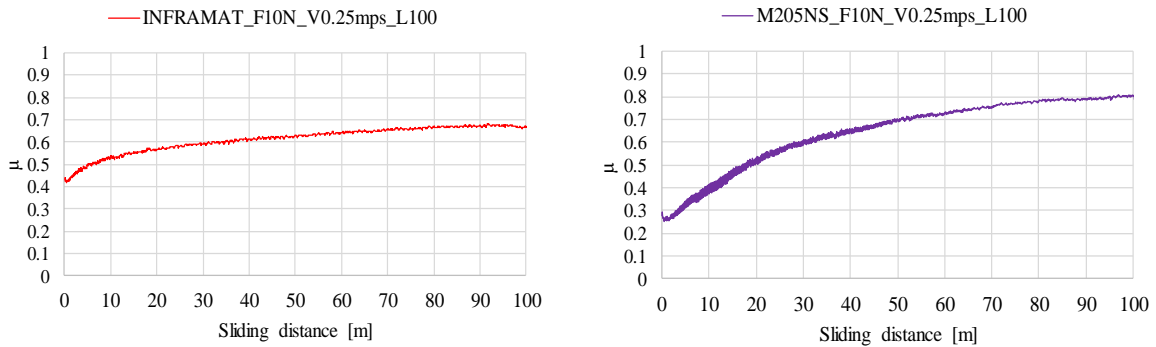


**Figure 2: Friction curves during the ball on disc test.**

For calculation of wear rate  $W_m$  was used formula Eq.1:

$$W_m = \frac{\Delta m(mg)}{F(N) * L(m)} \quad (1)$$

where  $\Delta m(mg)$  is mass loss at the end of the test,  $F(N)$  is normal applied force,  $L(m)$  is sliding distance. The results of wear rate are presented in Figure 2 and Figure 3. In this study was used the correlation of wear rate in order to underline the performances between coatings against steel ball.

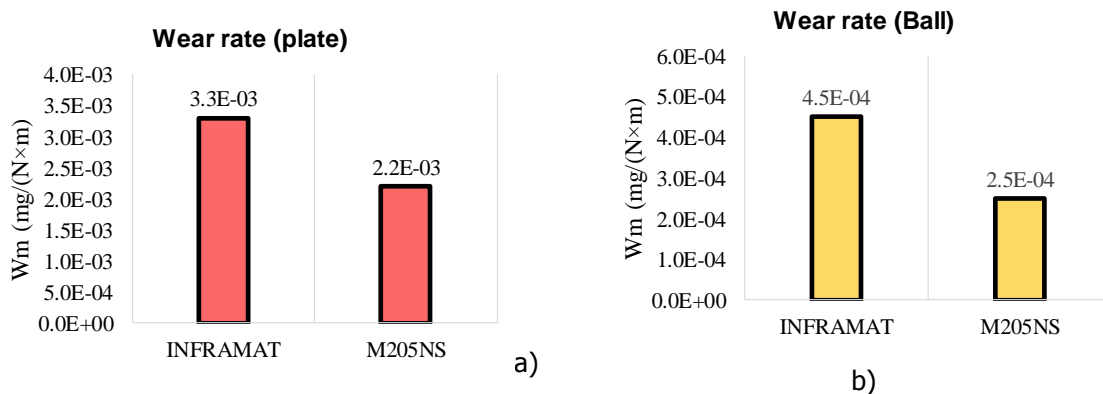


**Figure 3: Wear rate for a) coated plate b) steel ball.**

The average friction coefficients at the end of the test seems to be approximately the same for the investigated samples namely 0.60 for 7.5YSZ and 0.65 for CSZ. The differences can be seen in the shapes and the slope of the friction curves. The 7.5YSZ (INFRAMAT  $ZrO_2 7.5\% Y_2O_3$ ) present a smooth shape with small scattering values along the curve. It can be easily observed that 7.5YSZ friction curve starts almost from 0.4 friction coefficient value, leading to the conclusion that it has a strong abrasive surface. After 50 m of sliding distance, it was observed a stabilization of the friction coefficient around 0.62 and a maximum value of 0.69 at the end. Friction coefficient evolution along the test for M205NS ( $ZrO_2 25\% CeO_2 2.5\% Y_2O_3$  –CSZ), have an almost linear grow trend starting from 0.25 at the beginning, after 50 m of sliding the friction coefficient was  $\sim 0.70$ , the highest values for friction coefficient being around 0.82 at the end of the test (Figure 2). The tribological investigation present a lower massic wear rate of CSZ compared with YSZ.

### 3.2 Hardness testing

The Vickers hardness test method consists of indenting the test material with a diamond indenter, in the form of a right pyramid with a square base and an angle of 136 degrees between opposite faces subjected to a load. In this paper Vicker's micro-hardness ( $H_v$ ) was performed on the polished cross-section of the samples, with an indentation load of 1971N for 15 seconds by selecting 5 locations

randomly. The Vickers hardness is the quotient obtained by dividing the kgf load by the A, the surface area of the resulting indentation in square millimeter Eq.2.

$$H_V = \frac{F}{A} = \frac{2 \cdot F \cdot \sin\left(\frac{136^\circ}{2}\right)}{d^2} \quad [\text{kgf/mm}^2, \text{GPa}] \quad (2)$$

where F is load in kgf, A is the surface area of the resulting indentation in mm<sup>2</sup>, d is arithmetic mean of the two diagonals, d1 and d2 in mm. The Vicker's micro-hardness (H<sub>v</sub>) was performed on top coat, bond coat and Nimonic90 substrate. The results are presented in Table 4 and Table 5.

**Table 4: Vicker's micro-hardness for samples with 7.5YSZ.**

TC-(7.5YSZ) (H <sub>v</sub> 0.2)	BC- Amdry997 (H <sub>v</sub> 0.2)	Nimonic90 (H <sub>v</sub> 0.2)
244.4	189.6	169.6

**Table 5: Vicker's micro-hardness for samples with (CSZ).**

TC (CSZ) (H <sub>v</sub> 0.2)	BC-Amdry997 (H <sub>v</sub> 0.2)	Nimonic90 (H <sub>v</sub> 0.2)
218.8	173	165.4

Vicker's micro-hardness (H<sub>v</sub>) of CSZ is 229.8 (H<sub>v</sub> 0.2), smaller compared to YSZ 244.4 (H<sub>v</sub> 0.2). denoting and proving the poor behavior during the tribological tests of CSZ.

### 3.3 Thermal shock testing

Thermal shock tests were done on a research equipment designed and conceived by INCAS called QTS-2-(Quick Thermal Shock) [1], [2]. The purpose of the installation is to perform thermal shock tests, allowing a fast and economical method of quick ranking of the multilayered ceramic coating. Developed testing system and constantly upgraded equipment, ensures the reproducibility of the testing conditions by operating in semi-automatic regime. Functional parameters of the QTS-2 equipment are: maximum testing temperature – 1500°C, variable heating speed and quick cooling speed of tested specimen with an average up to 70°C/sec by compressed air and higher values achieved by new cryogenic cooling system. The installation is equipped with continuous temperature measurement pyrometers for specimen and oven during all thermal cycles steps. Temperatures variations are recorded and stored automatically by data acquisition under LabVIEW software. Coatings for thermal cycling test in this work are listed in Figure 4.

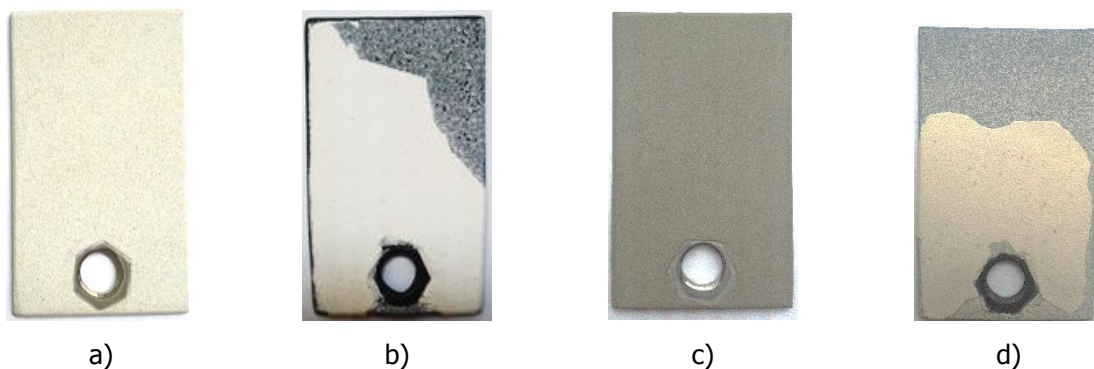


**Figure 4: a) YSZ sample before thermal shock, b) YSZ sample after 90 cycles, c) CSZ sample before thermal shock, d) CSZ sample after 75 cycles**

In this study, thermal shock cycles were done by exposing for 5 minutes to 1200°C and then cooled down by 8-9 bars compressed air for 1 minute using a 4mm nozzle at 35 mm distance from sample. Testing procedure for thermal shock is that the testing is terminated if a spallation of more than 20% of coated surface occurred. For the thermally tested samples coated with 7.5YSZ and CSZ, spallation for 7.5 YSZ occurred after 90 cycles and for CSZ after 75 thermal cycles.

### 3.4 Microstructure

Two different structural microstructures were observed in this study Figure 5 and Figure 6. They are mainly different for as coated morphostrucral surfaces.

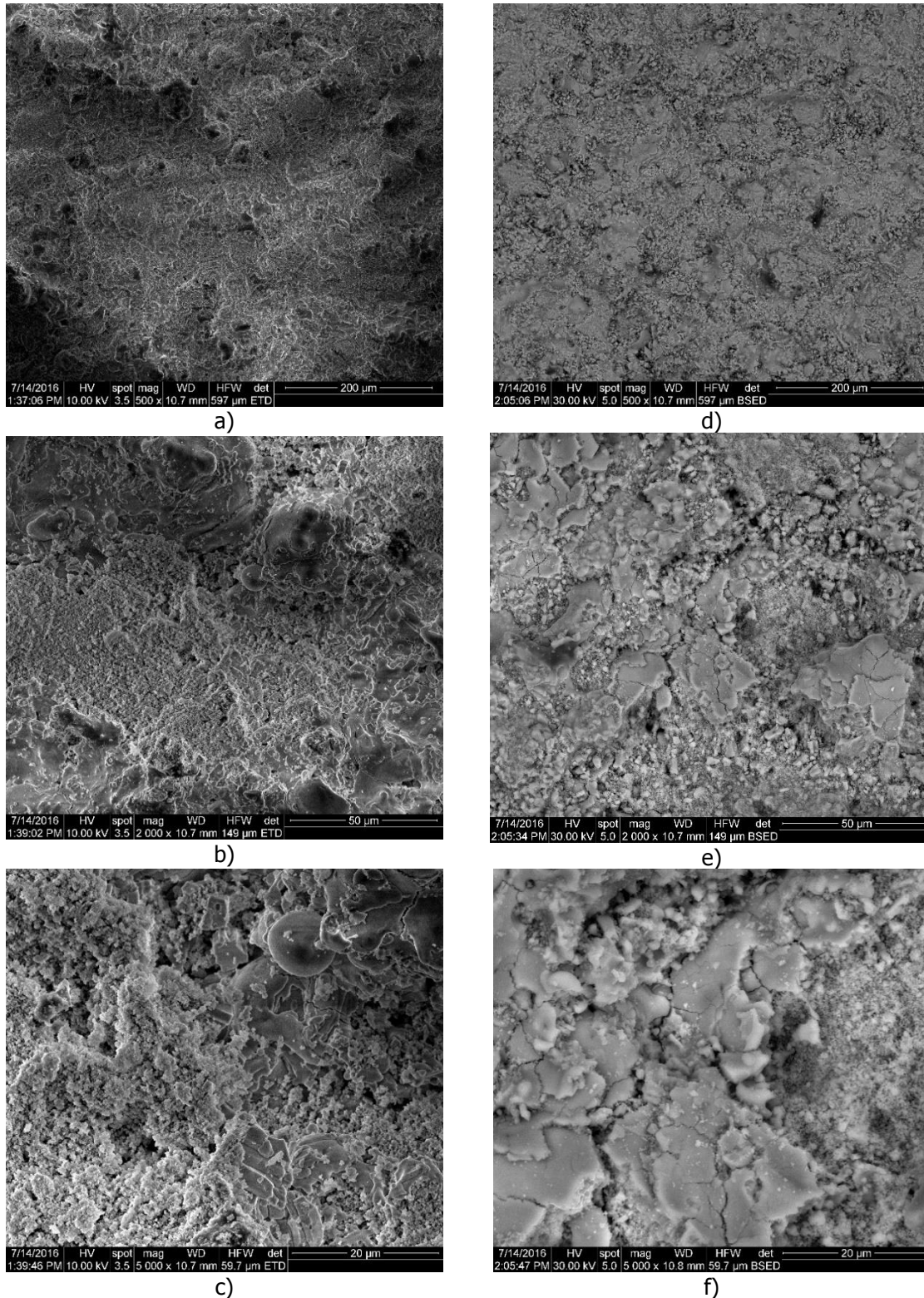


**Figure 5: SEM images of the surface for 7.5YSZ coating, a,b,c-before tribological testing, d,e,f-after tribological testing**

A prominent grainy surface for 7.5YSZ and with small splats on surface, leading to the formation of a melted stretched surface with nano recrystallized droplets on top, given the supersonic velocity of particles during coating process deposition Figure 5 a, b, c.

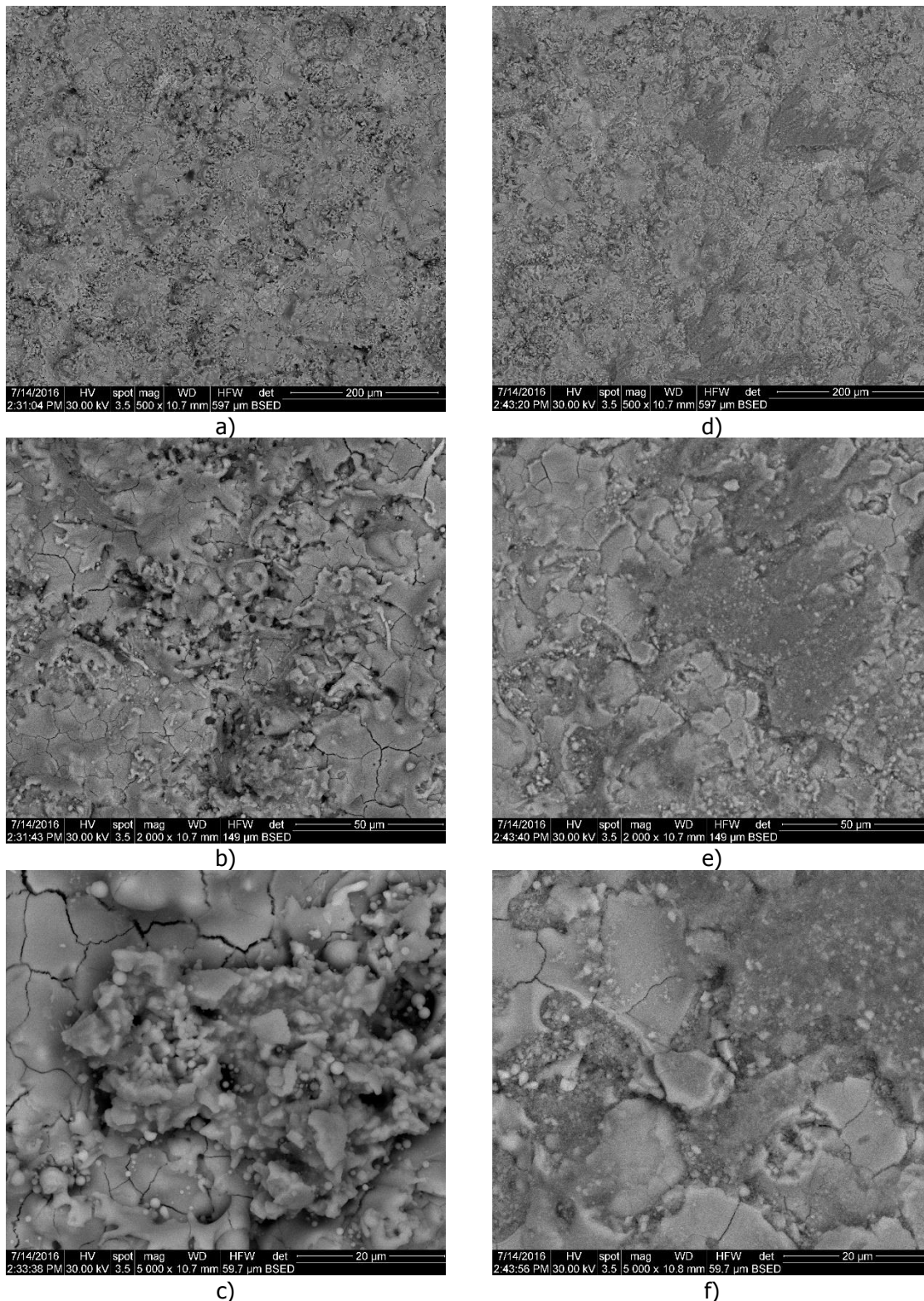


**Figure 6: SEM images of the surface for CSZ coating, a) before tribological testing, b) after tribological testing**

The SEM morphostrucral images for CSZ represent a cover with well melted particles, with large stretched droplets. The different from it others are observed in SEM images for CSZ coating Figure 6 a,



b, c, with represent a network of developed nano cracks on the surface, mostly on well melted stretched droplets. SEM images for 7.5 YSZ and CSZ after tribological testing are represented in Figure 5 d, e, f and Figure 6 d, e, f. The main conclusion on tribological evolution and microstructural consideration of coatings are that, a lower coefficient of friction was obtained for 7.5YSZ regarding the presence of nano grainy surface and removed during the test, living in contact with the steel ball the harder surface of melted droplets, conducting to a stabilization of the coefficient of friction YSZ (Figure 2).

In the case of CSZ, which was described with a well meted surface of the droplets but with a wide network of nano cracks, the contact of steel ball with the surface led to the segmentation of the surface created by nano cracks and then fragmentation. As the result of fragmentation, delamination of sharp splinters was leading to a higher coefficient of friction for CSZ and constantly growing of it during the test.

#### 4 Summary and conclusions

Plasma sprayed micro and nano-structural zirconia coatings were investigated under thermal shock and an evaluation of tribological and mechanical properties was performed. Tribological performances of coatings were investigated against stainless steel with a ball on disk testing procedure under dry friction conditions. Better wear performance of the nano-structured zirconia stabilized with yttria (7.5YSZ) is due the microstructure and mechanical properties enhancements compared with micro structured coating stabilized with ceria (CSZ). Advantages of nano-structured zirconia (7.5YSZ) coating were observed under thermal shock compared with ceria stabilized (CSZ) coating. The SEM structural investigation showed a complex microstructure. SEM images of plasma sprayed micro (CSZ) and nano (7.5YSZ) structured zirconia present well and partially melted splats and areas. A higher thermal shock resistance, tribological and mechanical properties was found on nano-structured zirconia coatings stabilized with yttria, this effect was correlated by nano structured areas in coating microstructure and the presence of melted splats. The main conclusion on tribological evolution and microstructural consideration of coatings are that the use of nano structured powders for coatings can bring improvements in the coefficient of friction and less nano cracks on the as coated surface. For the CSZ coating one shows a well meted surface but with a wide network of nano cracks resulting in segmentation and fragile fragmentation and splinters occurrence. This result reveals that the CSZ coating has a higher coefficient of friction and lower wear rate compared to 7.5YSZ.

#### Acknowledgement

The paper was prepared thanks to the Nucleus Program, contract no. PN 16 38 05 02 powered by UEFISCDI - Romanian Executive Agency for Higher Education, Research, Development and Innovation.

#### REFERENCES:

- [1] V. Manoliu, A. Mihailescu, G. Ionescu, and A. Stefan, "The behaviour of turbo engine associated thermal barrier coating structures from a tribological perspective.," *J. Int. Sci. Publ.*, vol. 9, pp. 269–278, 2015.
- [2] S. Dimitriu, V. Manoliu, G. Ionescu, and A. Stefan, "Multilayer Ceramic Materials Testing under the Terms of High Heating-Cooling Gradients," in *Advanced Materials Research*, 2015, vol. 1114, pp. 190–195.
- [3] X. Cao, "Development of New Thermal Barrier Coating Materials for Gas Turbines," Doctoral dissertation, Forschungszentrum Jülich in der Helmholtz-Gemeinschaft, 2004.
- [4] T. CUI, J. WANG, R. GUAN, L. Chen, and G. QIU, "Microstructures and Properties of Thermal Barrier Coatings Plasma-Sprayed by Nanostructured Zirconia," *J. Iron Steel Res. Int.*, vol. 14, no. 5, Supplement 1, pp. 116–120, 2007.
- [5] R. Vaßen, M. O. Jarligo, T. Steinke, D. E. Mack, and D. Stöver, "Overview on advanced thermal barrier coatings," *Surf. Coatings Technol.*, vol. 205, no. 4, pp. 938–942, 2010.
- [6] L. Pawlowski, *The Science and Engineering of Thermal Spray Coatings*. 2008.
- [7] B. Bernard *et al.*, "Thermal insulation properties of YSZ coatings: Suspension Plasma Spraying (SPS) versus Electron Beam Physical Vapor Deposition (EB-PVD) and Atmospheric Plasma Spraying (APS)," *Surf. Coatings Technol.*, vol. 318, pp. 122–128, 2017.
- [8] K. K. Szkaradek, "Thermal barrier ZrO<sub>2</sub>-Y<sub>2</sub>O<sub>3</sub> obtained by plasma spraying method and laser melting," *Manuf. Eng.*, vol. 17, no. 1, pp. 77–80, 2006.



- [9] S. Sodeoka, M. Suzuki, K. Ueno, H. Sakuramoto, T. Shibata, and M. Ando, "Thermal and Mechanical Properties of ZrO<sub>2</sub>-CeO<sub>2</sub> Plasma-Sprayed Coatings," *J. Therm. Spray Technol.*, vol. 6, no. September, pp. 361–367, 1997.
- [10] Y. Wang *et al.*, "Microstructural evolution of plasma sprayed submicron-/nano-zirconia-based thermal barrier coatings," *Appl. Surf. Sci.*, vol. 363, pp. 101–112, 2016.
- [11] H. Xu and H. Guo, *Thermal barrier coatings*, vol. 90, no. 8. Woodhead Publishing Limited, 2011.
- [12] Y. Zhang *et al.*, "Mechanical properties of zirconia composite ceramics," *Ceram. Int.*, vol. 39, no. 7, pp. 7595–7603, 2013.
- [13] "\*\*\*\*Material Product Data Sheet Ceria-Yttria Stabilized Zirconium Oxide."
- [14] "\*\*\*\*Material Product Data Sheet 8 % Yttria Stabilized Zirconia."
- [15] "\*\*\*\*<http://www.advancedmaterials.us/4039ON-8601.htm>."